Available online at www.sciencedirect.com

ScienceDirect

journal homepage: www.elsevier.com/locate/he

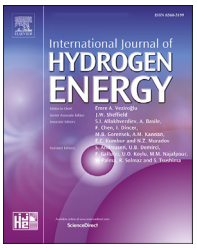

Computational analysis of an HCCI engine fuelled with hydrogen/hydrogen peroxide blends

Iliana D. Dimitrova [a], *Thanos Megaritis* [b], *Lionel Christopher Ganippa* [b], *Efstathios-Al Tingas* [c,*]

[a] Perth College, University of the Highlands and Islands, Crieff Rd, Perth PH1 2NX, United Kingdom
[b] College of Engineering Design and Physical Sciences, Brunel University London, Uxbridge UB8 3PH, United Kingdom
[c] School of Engineering and the Built Environment, Edinburgh Napier University, Edinburgh EH10 5DT, United Kingdom

HIGHLIGHTS

- Up to 10% H_2O_2 (/fuel vol) in H_2 is su_cient for HCCI engine operation at _eff = 0.1–0.4.
- H_2/H_2O_2 blends lead to much better engine performance compared to preheated H_2.
- Addition of H_2O_2 leads to increase of IMEP, torque, power and thermal e_ciency.
- Incremental addition of H_2O_2 results in decrease of NOx (no after-treatment required).

ARTICLE INFO

Article history:
Received 3 October 2021
Received in revised form
14 December 2021
Accepted 11 January 2022
Available online 3 February 2022

Keywords:
HCCI
Compression ignition engine
Heavy duty applications
Hydrogen engine
Dual fuel
Emissions

ABSTRACT

In the current work, Chemkin Pro's HCCI numerical model is used in order to explore the feasibility of using hydrogen in a dual fuel concept where hydrogen peroxide acts as ignition promoter. The analysis focuses on the engine performance characteristics, the combustion phasing and NOx emissions. It is shown that the use of hydrogen/hydrogen peroxide at extremely fuel lean conditions ($\varphi_{eff} = 0.1 - 0.4$) results in significantly better performance characteristics (up to 60% increase of IMEP and 80% decrease of NOx) compared to the case of a preheated hydrogen/air mixture that aims to simulate the use of a glow plug. It is also shown that the addition of H_2O_2 up to 10% (per fuel volume) increases significantly the IMEP, power, torque, thermal efficiency (reaching values more than 60%) while also decreasing remarkably NOx emissions which will not require any exhaust after-treatment, for all engine speeds. The results presented herein are novel and promising, yet further research is required to demonstrate the feasibility of the proposed technology.

Introduction

Hydrogen is considered one of the best candidates to replace fossil fuels for power generation and propulsion purposes, especially for applications that are hard to electrify such as marine propulsion and heavy duty vehicles [1,2]. The use of hydrogen in thermal engines is not novel and dates more than two centuries back but it wasn't until the seventies that

* *Corresponding author.*
E-mail address: e.tingas@napier.ac.uk (E.-A. Tingas).
https://doi.org/10.1016/j.ijhydene.2022.01.093

received increased interest due to the two energy crises that resulted in unprecedented increases of the oil prices and fuel shortages in many developed countries around the globe. Recently, it has attracted more interest again as an effective way to combat climate change. Although currently most hydrogen production relies on methane reforming (grey hydrogen), other techniques have also been developed, more environmentally friendly, allowing its production solely from renewable energy sources (green hydrogen) [3,4]. Nations like the United Kingdom and Japan have already pledged to the development of hydrogen-based strategies in their effort to decarbonise their societies [5,6].

Most research of hydrogen use in internal combustion engines (ICEs) has revolved around spark ignition (SI) engines. There is a vast literature on SI hydrogen engines which has been nicely summarised in many review works such as Refs. [7–12]. The great interest in SI hydrogen engines was not solely academic. In fact, large automakers such as Ford [13], DaimlerChrysler [14] and BMW [15] developed hydrogen fueled models. On the other hand, hydrogen use in compression ignition (CI) engines has not been particularly attractive and the reason has mainly to do with hydrogen's high autoignition temperature. In other words, the thermodynamic conditions reached in a conventional CI engine are not sufficient to trigger hydrogen's ignition. To tackle hydrogen's high resistance to autoignition, three strategies have been proposed. Firstly, the use of very high compression ratios (> 29:1), e.g. Ref. [16]. This approach is not attractive because it results to problems related to the mechanical strength of the engine structure, therefore, it requires an engine redesign. Secondly, the use of a glow plug with the purpose of preheating the intake air (e.g., Ref. [17]) and in few cases heating the hydrogen/air charge (e.g., Ref. [18]), therefore resembling to an SI engine operation. This technique is generally simple and has been tested both in conventional CI and homogeneous charge compression ignition (HCCI) engines, yet, the available literature of the last 30 years is scarce. Hydrogen combustion in CI/HCCI mode with the use of a glow plug has been reported to lead to very low NOx emissions where in some cases a three-way catalytic converted was not required [18–23]. In addition, such an approach has demonstrated higher fuel efficiency and power to weight ratio compared to the conventional, diesel-fueled mode [21]. Despite these promising results, the increase of the intake air temperature when used without any substantial modification of a conventional CI engine, leads to a decrease of the volumetric efficiency which results in the decrease of the indicated mean effective pressure (IMEP), the indicated thermal efficiency (ITE) and the brake thermal efficiency [19,20,22–24]. In HCCI mode, additional challenges relate to the limited operating range due to the high in-cylinder pressures reached and the difficulty in controlling the engine operation, the latter being an inherent characteristic of HCCI mode [19,20]. The third approach encompasses a dual fuel strategy, where the ignition of the in-cylinder charge is achieved by the direct injection of a more reactive fuel, e.g., diesel. This approach is particularly attractive, because it offers a unique flexibility in the engine operation while also maintaining (at least to some extend) the benefits from the CI/HCCI mode [25]. In CI/HCCI dual-fuel operation, hydrogen has been mainly used with carbon-based fuels, such as (bio-)diesel [26–28], natural gas [29,30] and others, with the only exceptions the work of Boretti on hydrogen/ammonia in a new engine design [31] and the work of Seignour et al. on hydrogen/ozone blends in HCCI mode [32]. Being carbon-based, the fuel blends produce carbonaceous emissions (e.g., CO_2) directly or indirectly (depending how these fuels are originally produced), thus, cancelling or reducing the efforts for drastic greenhouse gases (GHG) reduction.

Recently, an alternative approach was proposed, which relies on the use of hydrogen peroxide (H_2O_2) for the ignition promotion of H_2/air mixtures, accompanied by steam (H_2O) dilution for NOx reduction purposes, at CI-relevant conditions [33,34]. H_2O_2 has long been used as rocket propellant [35,36], while in conventional transport-related applications it has been used with a large variety of fuels for ignition advancement (e.g., Refs. [37,38]). In addition, steam dilution is a well-documented method of emissions reduction [39]. In the recent work of [33] it was reported that a mere 10% (per fuel volume) addition of H_2O_2 in H_2/air mixtures can lead to ignition delay times relevant to CI engines. Steam addition was also reported to induce a tremendous decrease in NOx emissions with a minimal detrimental impact on the ignition delay time. Furthermore, it was revealed that sufficient steam dilution of H_2/H_2O_2/air mixtures at fuel lean conditions can lead to a two-stage ignition. The latter is particularly important because it can facilitate the introduction of low temperature combustion (LTC) in hydrogen-fueled CI engines. Later, it was reported that H_2O_2 addition in H_2/air mixtures in the context of premixed laminar flames leads to a significant increase of the laminar flame speed, the heat release and NOx emissions, while also enhancing the stability of the flame and inducing a broadening of the reaction zone [34].

The results reported in Refs. [33,34] were obtained from the analysis of homogeneous batch reactor and laminar flame simulations, both idealized setups that are commonly used by the research community. These studies provided sufficient numerical evidence to justify the further exploration of the proposed technology in the context of numerical CI setups. The need for further numerical investigation stems from two facts: (i) none of the studies reported in Refs. [33,34] took into account the effect of H_2O_2/H_2O addition to the engine performance, and (ii) any follow up work with engine experiments will require a prior feasibility study which will provide some guidance to the design of the experiments. Therefore, the objective of the current work is to provide numerical evidence on the feasibility of the proposed technology of H_2/H_2O_2 blends in view of engine performance characteristics, NOx emissions and combustion phasing. For the analysis, a simplified HCCI engine model is used, that of the Chemkin Pro suite. The employed model is commonly used in the literature (e.g., Refs. [40–42]), however, the results have to be treated with care due to the simplifications that have been made and the assumptions that are considered. As a result, the purpose of the current work is to emphasize the qualitative features of the results and identify trends rather than highlighting quantitive aspects. The structure of the paper is as follows. Firstly, the HCCI engine model is briefly described along with the setup's engine details. Then the analysis follows which includes three parts. Firstly, the proposed technology of H_2/

H_2O_2/air is compared against preheated H_2/air mixtures. Secondly, the effect of the addition of H_2O_2 to H_2/air mixtures is investigated. Finally, the effect of H_2O_2 addition to H_2/air mixtures under constant (low and mild) load conditions is investigated.

Material and methods

The zero-dimensional single zone HCCI engine model of Chemkin Pro suite is used for all simulations performed in the current study. The model solves the species and energy equations plus an additional equation for volume to account for the piston movement. The latter is time-dependent (like the other governing equations) and is a function of engine parameters, including compression ratio, crank radius, connecting rod length, speed of revolution of the crank arm, and the clearance or displaced volume [43]. For more details about the mathematical formulation of the single zone HCCI engine model, the reader is referred to the manual of Chemkin Pro [44]. The model also considers that the system is fully closed, therefore, there is no mass exchange. In addition, for the purpose of the current study which aims at qualitative and not quantitative features of the results, the system is considered adiabatic therefore no heat losses are taken into account. Finally, the model considers that the mixture is fully homogeneous during throughout the simulation.

As shown in Table 1, the engine's bore and stroke are 10 and 10.5 cm, respectively. The engine compression ratio (CR) varies from 14 to 20 but the reference value is 17. Most of the investigation is performed at three engine speeds, 1,000, 2000 and 3000 rpm. Unless otherwise stated, the intake pressure (P_{in}) is 1 atm and the intake temperature (T_{in}) is 320 K. All simulations start at −180 crank angle degrees after top dead center (CAD aTDC) and end at 180 CAD aTDC. For consistency purposes with the previous works [33, 34], the chemical reaction mechanism of *Aramco 3* [45] was employed in the current study, supplemented with the nitrogen sub-mechanism of *Glarborg* et al. [46].

In the current work, hydrogen peroxide is added on the basis of the hydrogen mole fraction. Therefore, a 10% addition of H_2O_2 indicates that the H_2O_2 mole fraction ($X_{H_2O_2}$) is 10% of the hydrogen mole fraction (X_{H_2}), i.e., $X_{H_2O_2}/X_{H_2} = 10\%$. Since hydrogen peroxide can act as an oxidiser, the use of the conventional definition of equivalence ratio $\varphi = (X_F/X_{air})/(X_F/X_{air})_{st}$ is not suitable. Therefore, the definition of the effective equivalence ratio (φ_{eff}) is adopted, similar to the one introduced in Ref. [47] and in consistence with the previous work on hydrogen/hydrogen peroxide blends [34]. Therefore, the effective equivalence ratio is defined as:

$$\varphi_{eff} = \frac{X_{H_2}/(0.5X_{H_2O_2} + X_{O_2})}{(X_{H_2}/X_{O_2})_{st}} \quad (1)$$

where the subscript *st* denotes stoichiometric conditions. In principle, the definition assumes that 1 mol of H_2O_2 leads to the formation of 1 mol of H_2O and half mole of O_2. All simulations reported herein are performed at fuel lean conditions, mainly in the range of $0.1 \leq \varphi_{eff} \leq 0.4$, which are typical for hydrogen fueled HCCI engines [19,20,22,24,48,49].

In the following analysis, the indicated work is represented by $W_{c,i}$ following the same notation as in Chemkin's manual, and the indicated mean effective pressure IMEP is calculated from

$$IMEP = \frac{W_{c,i}}{V_{disp}} \quad (2)$$

where V_{disp} is the cylinder's displaced/swept volume, i.e., the volume swept by the piston defined as $V_{disp} = (\pi/2)D^2L_A$, where D the bore's diameter and $L_A = 36.8$ mm the crank arm radius. The indicated power is given from

$$P_i = \frac{W_{c,i}N}{2} \quad (3)$$

where N the engine speed in number of revolutions per second. Torque is defined as

$$T = \frac{P_i}{2\pi N} \quad (4)$$

while the indicated thermal efficiency is given by

$$n_{th} = \frac{1}{sfc \cdot Q_{HV}} \quad (5)$$

where *sfc* the specific fuel consumption defined as $sfc = (m_f N)/(2P_i)$, m_f the fuel mass in the initial gas charge and Q_{HV} is the heating value of the fuel.

Table 1 – HCCI engine specifications used in the simulations.

Engine speed	1000, 2000, 3000 rpm
Engine compression ratio	14–20
Bore	100 mm
Stroke	105 mm
Connecting Rod to Crank Radius Ratio	3.714 286
Intake pressure	1 atm
Intake temperature	320 K
Displaced/Swept volume	0.824 6 l

Results and discussion

First the analysis will focus on comparing the engine performance characteristics of two approaches: the proposed use of hydrogen/hydrogen peroxide blends against the sufficient preheating of hydrogen/air blends. This comparison is performed at 3 engine speeds (1,000, 2000 and 3000 rpm) and three equivalence ratios ($\varphi_{eff} = 0.1$, 0.2 and 0.3). The results of this comparison are displayed in Table 2 while Fig. 1 displays the pressure profiles of two of the examined cases. In essence, this comparison aims to highlight the theoretical advantages of the proposed technology (i.e., that of hydrogen/hydrogen peroxide blends) against the more conventional approach of the charge preheating with a glow plug. The cases were set up as follows. Starting at $\varphi_{eff} = 0.1$ and 1000 rpm, the charge includes only hydrogen and air (i.e., 0% H_2O_2) and the intake temperature is incrementally increased until the ignition CAD reaches a value of between +1 and + 2, i.e., 1 aTDC < CAD_{ign} < 2 aTDC (the only exception is the case of $\varphi_{eff} = 0.1$ and 3000 rpm where $CAD_{ign} \approx 4$ CAD aTDC). It is noted that the ignition CAD is defined on the basis of the

Table 2 – Engine performance results for various cases of engine speed (1000, 2000, 3000 rpm) and mixture effective equivalence ratio ($\varphi_{eff} = 0.1, 0.2, 0.3$) with and without H_2O_2 addition. The percentage of H_2O_2 addition refers to the H_2 mole fraction. The ignition CAD are determined on the basis of the maximum temperature rate of change. CAD90 represents the CAD where 90% of the heat release rate have been reached. n_{th} represents the thermal efficiency. NOx emission values have units of ppmvd and represent the gas-phase volumetric fraction of NOx expressed in parts per million, after removing the volumetric contribution of water. For each case of 0% H_2O_2 a case with the addition of H_2O_2 is shown, maintaining the ignition CAD constant. All cases with the addition of H_2O_2 have $T_{in} = 320$ K. In all cases (with and without H_2O_2) the ignition CAD is maintained at 1–2 CADs aTDC, with the only exception of $\varphi_{eff} = 0.1$ and 3000 rpm where $CAD_{ign} \approx 4$ aTDC.

	Speed	% H2O2	T_{in}	CAD_{ign}	CAD90	IMEP	Power	Torque	n_{th}	T_{max}	NOx	P_{max}
	Rpm		K	CAD aTDC	CAD aTDC	bar	J/sec	N · m		K	Ppmvd	bar
φ_{eff}=0.1	1000	0.00%	386.1	1.89	2.02	2.12	1458.1	13.9	0.609	1462.7	0.33	67.5
	1000	12.00%	320.0	1.89	4.32	2.75	1891.5	18.1	0.618	1301.3	0.11	70.5
	2000	0.00%	401.4	1.97	2.13	2.03	2791.6	13.3	0.607	1496.0	0.39	66.3
	2000	28.00%	320.0	1.97	4.54	2.96	4071.2	19.4	0.618	1316.6	0.11	71.4
	3000	0.00%	407.3	3.95	4.16	1.99	4109.2	13.1	0.604	1498.3	0.40	64.0
	3000	40.00%	320.0	3.97	6.65	3.09	6374.9	20.3	0.612	1309.4	0.09	69.5
φ_{eff}=0.2	1000	0.00%	374.9	1.84	1.84	4.11	2824.0	27.0	0.596	1779.7	1.21	83.3
	1000	4.25%	320.0	1.84	1.85	5.01	3441.4	32.9	0.606	1672.2	0.81	91.8
	2000	0.00%	390.3	1.69	1.69	3.93	5402.4	25.8	0.594	1812.7	1.43	81.5
	2000	10.00%	320.0	1.70	1.71	5.17	7102.7	33.9	0.607	1688.2	0.92	92.9
	3000	0.00%	399.2	1.85	1.85	3.83	7901.1	25.2	0.592	1831.0	1.57	80.4
	3000	17.00%	320.0	1.86	1.87	5.36	11 055.7	35.2	0.607	1707.1	1.00	94.1
φ_{eff}=0.3	1000	0.00%	369.3	1.49	1.49	5.89	4051.0	38.7	0.583	2068.3	78.68	96.7
	1000	2.50%	320.0	1.49	1.49	7.00	4811.8	45.9	0.592	1975.6	18.51	106.7
	2000	0.00%	383.5	1.75	1.75	5.65	7768.7	37.1	0.581	2096.8	56.15	94.3
	2000	5.50%	320.0	1.75	1.75	7.12	9791.7	46.8	0.591	1986.8	9.97	107.3
	3000	0.00%	393.0	1.51	1.51	5.50	11 341.0	36.1	0.579	2116.5	50.11	92.9
	3000	9.50%	320.0	1.52	1.52	7.29	15 031.9	47.8	0.591	2002.8	8.73	108.5

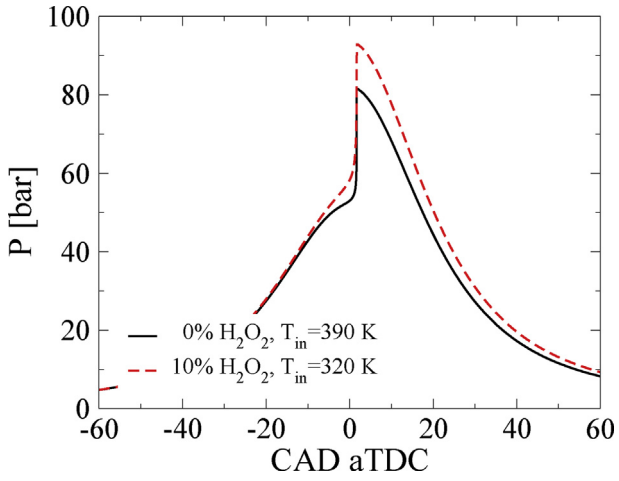

Fig. 1 – The in-cylinder pressure profile of a simulated HCCI engine for the cases of 0% H_2O_2, $T_{in} = 390$ K and 10% H_2O_2, $T_{in} = 320$ K. In both cases $P_{in} = 1$ atm and $\varphi_{eff} = 0.2$. The difference of the ignition CAD (on the basis of the maximum temperature rate of change) between the two cases is less than 1%.

maximum temperature rate of change. Then, the intake temperature is set to 320 K and the initial hydrogen peroxide content in the initial fuel/air mixture is incrementally increased, while maintaining the effective equivalence ratio constant at 0.1. The case of % H_2O_2 addition that achieves the same CAD_{ign} is then compared against the one with no H_2O_2. This process is repeated for the three aforementioned effective equivalence ratios and engine speeds.

In detail, at $\varphi_{eff} = 0.1$, the required increases of the intake temperatures to achieve the desired ignition CAD are 66, 81 and 87 K at engine speeds of 1000, 2000 and 3000 rpm, respectively. On the other hand, through the addition of H_2O_2, the desired outcome is achieved with 12, 28 and 40% of H_2O_2 at 1,000, 2000 and 3000 rpm, respectively. Table 2 shows that the addition of H_2O_2 leads to the: (i) significant increase of the IMEP, ranging between 29% to 55%, (ii) significant increase of the indicated power similar in magnitude to the IMEP, (iii) significant increase of the torque similar in magnitude to the IMEP, (iv) small (~1.5%) increase of the thermal efficiency, (v) notable decrease of the maximum temperature by 11%–13%, (vi) tremendous decrease of NOx emissions by 67%–78% and (vii) insignificant increase of the maximum pressure by 4%–9%. All the aforementioned findings, except for the last one, demonstrate the advantageous character of the use of hydrogen peroxide for ignition promotion instead of the pre-heating the charge. The increases similar in magnitude of the IMEP, indicated power and torque are all related to the increase of the indicated work. The thermal efficiency is a function of two quantities: the specific fuel consumption and the heating value of the fuel. With the addition of H_2O_2, the first increases significantly because of the much higher molecular weight of H_2O_2 (34 g/mol for H_2O_2 vs 2 g/mol for H_2) which leads to a much higher fuel mass, while the latter decreases greatly because of the much lower heating value of H_2O_2 (3 kJ/g for H_2O_2 vs 120 kJ/g for H_2). Hence, this cancellation of the specific fuel consumption with the fuel heating value leads to a minimal increase of the indicated thermal efficiency. NOx emissions are generally too low with 0% H_2O_2 but with the addition of H_2O_2 and the associated decrease of the intake temperature, the maximum temperature drops and

this results in decreased production of NOx emissions. Finally, the notable increase of the maximum pressure due to the addition of H_2O_2 should be highlighted as one of the issues that would potentially need to be addressed by alternative approaches such as steam addition.

At $\varphi_{eff} = 0.2$, the required amount of H_2O_2 to achieve the same ignition CAD as the preheated case of no H_2O_2, drop significantly compared to the cases reported for $\varphi_{eff} = 0.1$. In particular, 4.25, 10 and 17% of H_2O_2 are required at 1,000, 2000 and 3000 rpm, respectively, compensating the effect of respective increases of the intake temperature of 55, 70 and 79 K. The addition of H_2O_2 has the same effect on the engine performance characteristics as previously discussed for $\varphi_{eff} = 0.1$: important increase of IMEP, power and torque, small increase of the thermal efficiency, great decrease of the maximum temperature and NOx emissions and insignificant increase of the maximum pressure. However, the increase of IMEP, power and torque now ranges between 22% and 40% (compared to 29%–55% increase at $\varphi_{eff} = 0.1$), the increase of the thermal efficiency becomes slightly more pronounced ranging between 1.7% and 2.5% (compared to ~1.5% increase at $\varphi_{eff} = 0.1$), the decrease of the maximum temperature becomes less pronounced (6%–7% compared to 11%–13% decrease at $\varphi_{eff} = 0.1$), the decrease of NOx emissions becomes less prominent ranging between 33% and 36% (compared to 67%–78% decrease at $\varphi_{eff} = 0.1$) and the increase of the maximum pressure becomes more striking ranging between 10% and 17% (compared to 4%–9% increase at $\varphi_{eff} = 0.1$).

By increasing further the effective equivalence ratio, at $\varphi_{eff} = 0.3$, the system becomes more sensitive to the addition of H_2O_2; the required amount of H_2O_2 to achieve the same ignition CAD as with preheated charge now ranges between 2.5 and 9.5%. In essence, the required amount of H_2O_2 at constant speed drops an order of magnitude when moving from $\varphi_{eff} = 0.1$ to $\varphi_{eff} = 0.3$. For instance, at 1000 rpm and $\varphi_{eff} = 0.1$ the required amount of H_2O_2 is 12% while at $\varphi_{eff} = 0.3$, the respective amount is merely 2.5%. At $\varphi_{eff} = 0.3$, the addition of H_2O_2 induces the same changes on the engine performance characteristics as those previously reported for $\varphi_{eff} = 0.1$ and 0.2. In fact, the IMEP, power and torque still increase with the addition of H_2O_2, however, their increase becomes less pronounced following the trend identified at $\varphi_{eff} = 0.2$, i.e., it now ranges between 19% and 33%. The thermal efficiency is still marginally increased with the addition of H_2O_2, with an increase of 1.5%–2%, as previously reported for $\varphi_{eff} = 0.1$ and 0.2. The maximum temperature drops by ~5% (following the trend of becoming less pronounced as the mixture gets richer), however, NOx emissions both drop significantly by 77%–83%. The reason that NOx emissions decrease does not follow a clear trend as the mixture becomes richer (from $\varphi_{eff} = 0.1$ to 0.2 the decrease becomes less striking while from $\varphi_{eff} = 0.2$ to 0.3 it increases) is attributed to the fact that at sufficiently lean conditions ($\varphi_{eff} = 0.1$ to 0.2) the maximum temperature is quite low therefore the NOx production pathway remains largely inactive. However, as the mixture becomes richer the system reaches temperatures which start to activate the NOx production pathway and even small changes to the temperature will have significant effect on NOx production. Finally, the maximum pressure 10%–17% increases at levels similar to those described for $\varphi_{eff} = 0.2$.

In summary, the comparison of the two strategies of hydrogen peroxide addition versus the preheating of the charge indicates that the first approach is more advantageous compared to the latter because it leads to significantly enhanced engine performance (higher IMEP, power and torque) and reduced NOx. However, as the mixture becomes richer, the increase on the engine performance characteristics becomes less pronounced while the decrease of NOx emissions is maintained high. In addition, the hydrogen peroxide addition leads to a small increase of the thermal efficiency, which is maintained low regardless the mixture's effective equivalence ratio. Finally, an issue of potential concern is the maximum pressure increase induced by the addition of H_2O_2, which could be addressed by steam addition or other counter-pressure-rise strategies.

Next, the analysis will consider the effect of the addition of H_2O_2 on the engine performance characteristics, combustion phasing and NOx emissions, at constant engine speed (1000, 2000 and 3000 rpm) and effective equivalence ratio conditions ($\varphi_{eff} = 0.1, 0.2, 0.3, 0.4$). Starting with the combustion phasing, Fig. 2 shows the variation of the ignition CAD (based on the maximum rate of change of temperature) and the rapid burn angle (defined as the CAD between 10% and 90% of the heat release rate) as a function of H_2O_2 addition. Firstly, Fig. 2a–c shows that the addition of H_2O_2 results initially in drastic reduction of the ignition CAD and further addition has negligible effect on the ignition promotion, therefore, the CAD_{ign} levels off. This profile becomes attenuated at very lean conditions, i.e., $\varphi_{eff} = 0.1$, and in fact as the engine speed increases the dependence of CAD_{ign} on the H_2O_2 becomes roughly linear. In essence, Fig. 2 shows that as the mixture becomes richer (i.e., as the effective equivalence ratio increases) and regardless the engine speed, the effect of H_2O_2 addition on the ignition promotion becomes more pronounced. For instance, at 1000 rpm and $\varphi_{eff} = 0.4$ a mere 2% addition of H_2O_2 induces 0 CAD_{ign} aTDC while the required amount to achieve the same CAD_{ign} aTDC at $\varphi_{eff} = 0.1$ increases to ~15%. In fact, mixtures of $\varphi_{eff} = 0.1$ require significantly higher H_2O_2 content compared to the other effective equivalence ratios to achieve comparable results of CAD_{ign}. Even so, at 1000 rpm a mixture of $\varphi_{eff} = 0.1$ and 10% H_2O_2 would have ~4 CAD_{ign} aTDC, which is ideal for an HCCI engine. At 2000 rpm and $\varphi_{eff} = 0.2$, 10% H_2O_2 addition induces ~2 CAD_{ign} aTDC and at 3000 rpm and $\varphi_{eff} = 0.3$ the same percentage of H_2O_2 leads to ~1 CAD_{ign} aTDC. These results indicate that from a combustion phasing point of view, the addition of ~10% H_2O_2 could enable the engine operation at very lean conditions ($0.1 \leq \varphi_{eff} \leq 0.3$) in a wide range of engine speeds. At slightly higher effective equivalence ratios, i.e., $\varphi_{eff} = 0.4$, the required percentage of H_2O_2 to achieve CAD_{ign} in the range of 0–4 CAD aTDC drops significantly, and a mere 5% could enable the engine operation at all engine speeds under investigation.

Another important aspect of combustion phasing is that of the rapid burn angle, i.e., the degrees required for the heat release rate to increase from 10% to 90%. Fig. 2d–f shows that at all equivalence ratios except for $\varphi_{eff} = 0.1$, the addition of H_2O_2 results initially in a fast decrease of the rapid burn angle which eventually levels off and reaches an asymptotic limit close to ~0 CAD. At $\varphi_{eff} = 0.1$, the system's response, in view of the rapid burn angle, to H_2O_2 addition is significantly less

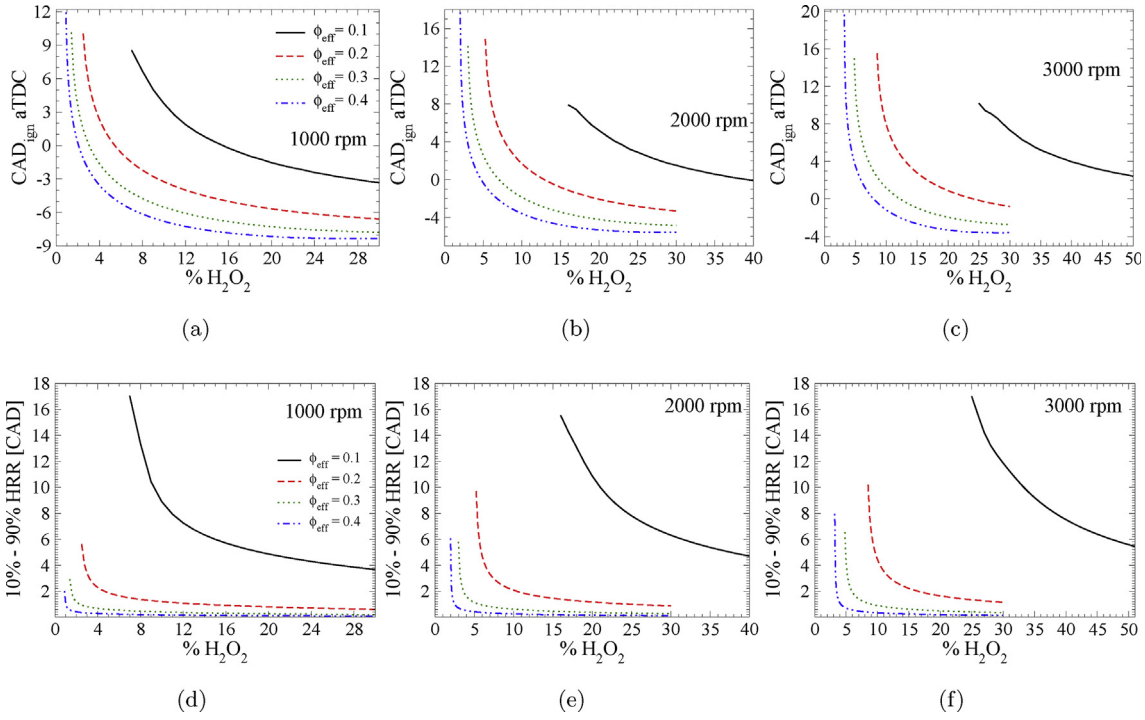

Fig. 2 – The variation of the ignition CAD (on the basis of the maximum temperature rate of change) and the rapid burn angle (the CAD for 10%–90% heat release rate) as a function of the H_2O_2 addition, for engine speed of (a, d) 1000, (b, e) 2000 and (c, f) 3000 rpm and equivalence ratios of $\varphi = 0.1$, 0.2, 0.3 and 0.4. The percentage of H_2O_2 addition refers to the H_2 mole fraction.

sensitive, in agreement with the findings previously reported for the CAD_{ign}.

Following the same practice as in Ref. [19], the minimum quantity of H_2O_2 required to sustain the rapid burn angle at 4 CAD or less is determined and the results are displayed in Fig. 3 for the three engine speeds. In essence, Fig. 3 echoes the message of Fig. 2 in that the effect of H_2O_2 addition on the combustion phasing becomes significantly less pronounced as the system becomes leaner and particularly at $\varphi_{eff} = 0.1$. At all engine speeds and for φ_{eff} = 0.2, 0.3, 0.4, a ~10% (or less) addition of H_2O_2 guarantees that the rapid burn angle will be less or equal to 4 CAD. On the other hand, at $\varphi_{eff} = 0.1$ the required amount of H_2O_2 to sustain 4 CAD of the rapid burn angle increases to 26% and 47% for 1000 and 2000 rpm, respectively, while at 3000 rpm the required amount of H_2O_2 exceeded 60%.

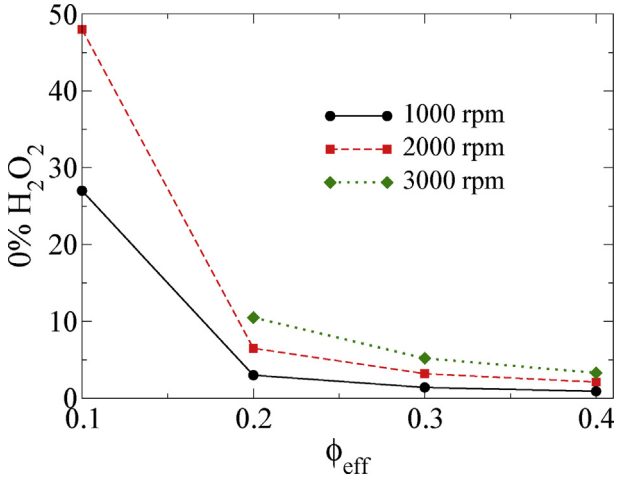

Fig. 3 – The variation of the required H_2O_2 addition to sustain 4 CAD for the rapid burn angle as a function of the effective equivalence ratio (φ_{eff}), at 1000, 2000 and 3000 rpm engine speed. The percentage of H_2O_2 addition refers to the H_2 mole fraction.

Next, the analysis focuses on the engine performance characteristics and in particular, the IMEP, power, torque and thermal efficiency and the results are displayed in Figs. 4–6. Starting with Fig. 4 it is evident that the addition of H_2O_2 increases the IMEP, power, torque for all engine speeds and effective equivalence ratios. In fact, the change that H_2O_2 induces to these quantities seems to be generally linear. Indicatively: (i) at 1000 rpm, φ_{eff} = 0.1 and 10% H_2O_2, the IMEP is 2.7 bar, P_i = 1855 W and T = 17.7 N•m; (ii) at 1000 rpm, φ_{eff} = 0.2 and 10% H_2O_2, the IMEP is 5.2 bar, P_i = 3557 W and T = 33.9 N•m; (iii) at 2000 rpm, φ_{eff} = 0.3 and 10% H_2O_2, the IMEP is 7.3 bar, P_i = 10,040 W and T = 47.9 N•m; (iv) at 3000 rpm, φ_{eff} = 0.4 and 10% H_2O_2, the IMEP is 9.2 bar, P_i = 18,977 W and T = 60.4 N•m. Exploiting the strongly linear character that the results of IMEP, torque and power present for the most range of H_2O_2 addition, a linear regression analysis was performed with the purpose of determining the gradients of the respective lines. Considering that the larger the gradient of a line the larger the change on the y-axis, this analysis aims at assessing the overall sensitivity of the engine performance characteristics under discussion due to the

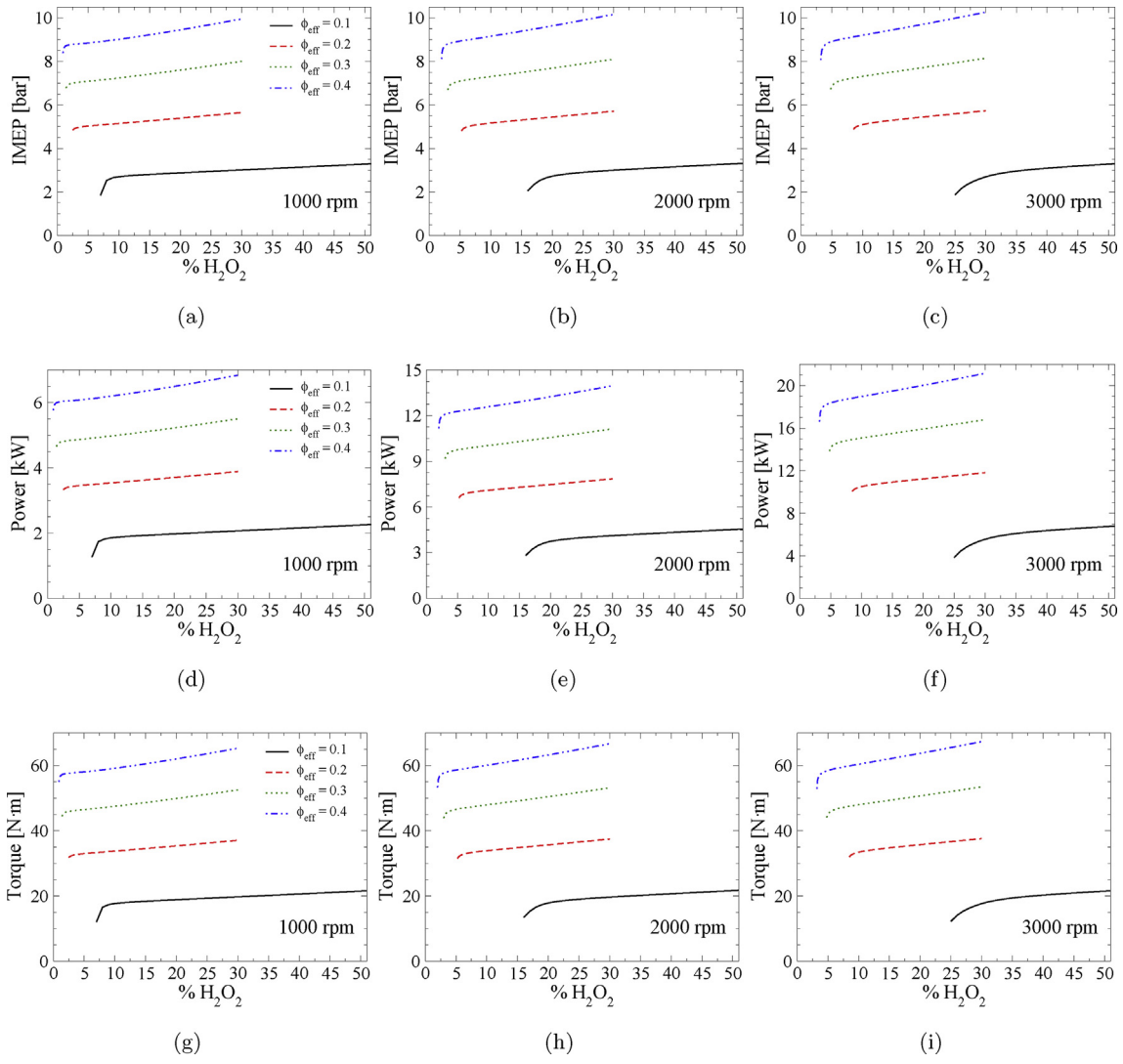

Fig. 4 – The variation of IMEP (a–c), power (d–f) and torque (g–i) as a function of the H_2O_2 addition, for engine speed of 1000 (a, d, g), 2000 (b, e, h) and 3000 (c, f, i) rpm and equivalence ratios of φ = 0.1, 0.2, 0.3 and 0.4. The percentage of H_2O_2 addition refers to the H_2 mole fraction.

addition of H_2O_2. For IMEP, the linear regression at 1000 rpm produced gradients of 1.375, 2.4709, 3.5691 and 4.3009 for φ_{eff} = 0.1, 0.2, 0.3 and 0.4, respectively. These results indicate an 80% increase of the IMEP gradient from φ_{eff} = 0.1 to 0.2, a 44% increase from φ_{eff} = 0.2 to 0.3 and a 21% increase from φ_{eff} = 0.3 to 0.4. Therefore, as the mixture becomes richer the gradient increases at a gradually smaller rate. Similarly, at 2000 rpm the linear regression produced gradients of 1.7109, 2.7716, 3.9609 and 4.8417 for φ_{eff} = 0.1, 0.2, 0.3 and 0.4, respectively, thereby indicating a 62% increase from φ_{eff} = 0.1 to 0.2, a 43% increase from φ_{eff} = 0.2 to 0.3 and a 22% increase from φ_{eff} = 0.3 to 0.4. Finally, at 3000 rpm the produced gradients were 2.0174, 3.082, 4.2632 and 5.3292 for φ_{eff} = 0.1, 0.2, 0.3 and 0.4, respectively, suggesting a 53% increase from φ_{eff} = 0.1 to 0.2, a 38% increase from φ_{eff} = 0.2 to 0.3 and a 25% increase from φ_{eff} = 0.3 to 0.4. The key message in this analysis is that as the mixture becomes richer the effect of H_2O_2 addition on IMEP, power and torque becomes stronger at a gradually smaller rate. Also, the difference between φ_{eff} = 0.1 to 0.2 in the effect of H_2O_2 addition on IMEP, power and torque is significantly larger when compared to the respective changes between φ_{eff} = 0.2 and 0.3 or φ_{eff} = 0.3 to 0.4.

The effect of H_2O_2 addition on the thermal efficiency is displayed in Fig. 5. Firstly, it is shown that the thermal efficiency generally drops with the increase of the φ_{eff}. It is reminded that the thermal efficiency is a function of the specific fuel consumption (*sfc*) and the heating value of the fuel blend (Q_{HV}). When φ_{eff} increases, for the same % of H_2O_2, both the Q_{HV} and *sfc* increase, which result in the decrease of n_{th}. Secondly, with the H_2O_2 addition, n_{th} initially rapidly increases and reaches the highest value and then gradually decreases. This is reasonable considering the ignition advancement induced by the addition of H_2O_2, as shown in Fig. 5d–e; the initial addition of H_2O_2 has a strong effect on the ignition advancement which is gradually reduced and quickly reaches 0 CAD aTDC. At that point the system reaches the maximum n_{th}. Further addition of H_2O_2 promotes ignition to values lower than 0 CAD aTDC which has an adverse effect on

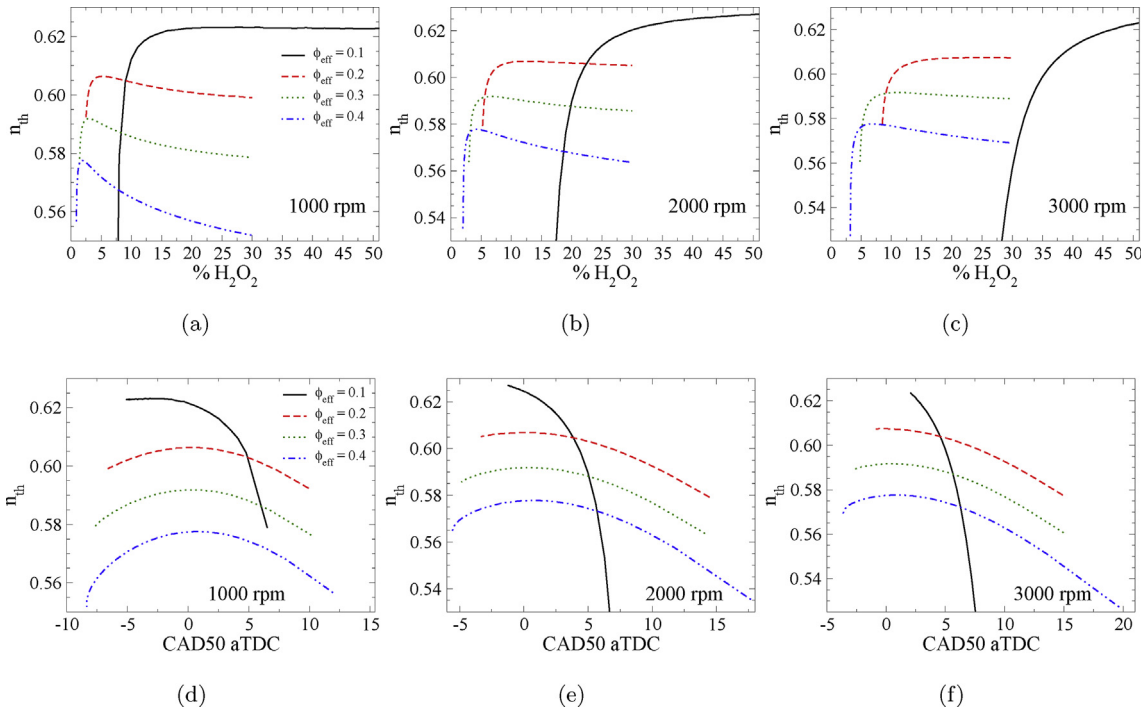

Fig. 5 – The variation of the thermal efficiency as a function of the H_2O_2 addition (a–c), and CAD50 (d–f) for engine speed of 1000 (a, d), 2000 (b, e) and 3000 (c, f) rpm and equivalence ratios of $\varphi = 0.1$, 0.2, 0.3 and 0.4. The percentage of H_2O_2 addition refers to the H_2 mole fraction.

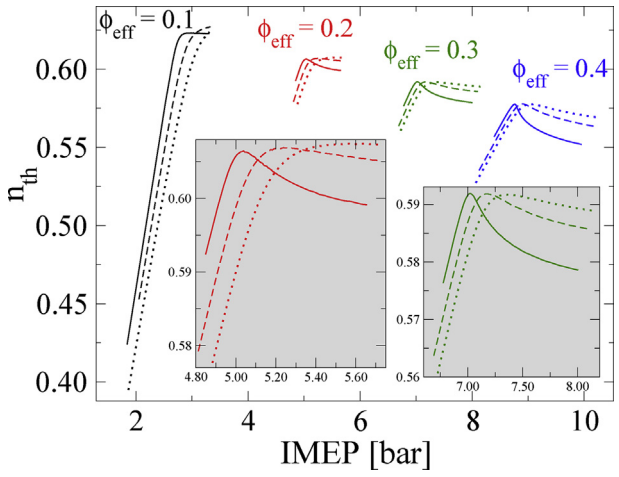

Fig. 6 – The variation of the IMEP against the thermal efficiency while maintaining constant the effective equivalence ratio ($\varphi_{eff} = 0.1$, 0.2, 0.3 and 0.4). The change in load is controlled by the percentage addition of H_2O_2. Results are presented for engine speed of 1000 (solid lines), 2000 (dashed lines) and 3000 (dotted lines) rpm. The percentage of H_2O_2 addition refers to the H_2 mole fraction.

n_{th}. At 1000 rpm, the maximum thermal efficiencies reached are 0.623 2 (31.00% H_2O_2), 0.606 4 (5.25% H_2O_2), 0.591 8 (3.00% H_2O_2), 0.577 6 (1.90% H_2O_2) for φ_{eff} = 0.1, 0.2, 0.3 and 0.4, respectively. At 2000 rpm the maximum values slightly increase and become 0.627 0 (50.00% H_2O_2), 0.606 9 (12.75% H_2O_2), 0.591 8 (6.80% H_2O_2), 0.577 8 (4.20% H_2O_2) for φ_{eff} = 0.1, 0.2, 0.3 and 0.4, respectively. At 3000 rpm, only $\varphi_{eff} = 0.2$ exhibits some small further increase of the maximum thermal efficiency with a value of 0.607 4 (24.00% H_2O_2). The rest φ_{eff} cases remain practically the same as in 2000 rpm. In any case, the important conclusions drawn here are that the addition of H_2O_2 tends to increase the system's thermal efficiency, regardless the engine speed and the effective equivalence ratio, and the thermal efficiency can exceed values of 60% at sufficiently lean conditions.

Fig. 6 further compares the variation of the thermal efficiency against IMEP for various engine speeds, while maintaining constant the effective equivalence ratio at φ_{eff} = 0.1, 0.2, 0.3 and 0.4. The variation in the load is achieved by varying the percentage addition of H_2O_2. Firstly, it is can observed that the engine speed has practically no effect on the load range for all four φ_{eff} values. Secondly, the maximum thermal efficiency for each case of φ_{eff} and engine speed does not coincide with the maximum load value. This is due to the enhanced ignition advancement that is achieved by the addition of H_2O_2, which promotes the ignition occurrence to CAD before the TDC. Thirdly, at constant φ_{eff} and low loads, the engine speed appears to move the line to the right, i. e, the same efficiency is achieved by the same IMEP difference between two speeds. This justifies why at constant φ_{eff} the same thermal efficiency is achieved at all engine speeds with monotonically increasing with engine speed values of IMEP. However, while the engine load is increased further (beyond the threshold corresponding to the maximum thermal efficiency) and the thermal efficiency starts dropping at constant φ_{eff}, there is great variation in the response of the thermal efficiency due to the engine speed. For example, at φ_{eff} = 0.4 and IMEP = 9.5, n_{th} = 0.556,

0.569 and 0.574 for engine speeds of 1,000, 2000 and 3000 rpm, respectively. The load and the thermal efficiency values reported herein are significantly higher than those reported in the earlier work of [19] that achieved experimentally hydrogen use in HCCI mode with appropriate preheating of the charge.

An important aspect in hydrogen-fueled engines that requires special attention is that of NOx emissions which can become quite high especially when compared with conventional fossil fuels. Fig. 7 displays the variation of exhaust NOx emissions against H_2O_2 addition in units of dry ppm basis, at $\varphi = 0.1$, 0.2, 0.3 and 0.4 and engine speeds of 1,000, 2000 and 3000 rpm. At sufficiently low effective equivalence ratios, e.g., $\varphi_{eff} = 0.1$ or 0.2, NOx emissions are so low that would not require any after-treatment. In fact for $\varphi_{eff} \leq 0.2$ NOx emissions are less than 1.5 ppmvd at all engine speeds. However, above $\varphi_{eff} = 0.2$ NOx emissions increase rapidly and reach values which may necessitate after-treatment or the use of additional strategies to combat the increased emissions, such as the use water/steam. For instance, at 1000 rpm and 10% H_2O_2, NOx emissions are 0.09, 0.99, 90.6 and 4279 ppmvd for $\varphi_{eff} = 0.1$, 0.2, 0.3 and 0.4, respectively. The main reason for the decreased NOx emissions at sufficiently low φ_{eff} values is the low maximum temperatures reached by the system, as illustrated in Fig. 7a–c. At $\varphi_{eff} = 0.1$, all maximum temperatures reached for the various cases of addition of H_2O_2 do not exceed the 1384 K. Similarly, at $\varphi_{eff} = 0.2$ the 1750 K. However, at $\varphi_{eff} = 0.3$ and 0.4, the maximum temperatures reach values of 2096 and 2395 K, respectively. Therefore, the system would benefit from steam addition with respect to the reduction of NOx emissions only for values of $\varphi_{eff} > 0.2$. Notice also that at $\varphi_{eff} = 0.3$ and 0.4, NOx emissions increase with the addition of H_2O_2 as opposed to $\varphi_{eff} = 0.1$ and 0.2 where the system seems to reach quickly an asymptotic value.

All the previous analysis considered engine operation with compression ratio of 17. Next, the effect of H_2O_2 addition on the combustion phasing, the engine performance and NOx emissions is explored in a range of compression ratios (15–20). Fig. 8 displays the variation of the minimum percentage of H_2O_2 addition to achieve thermal efficiency at the 98% of the maximum efficiency reached by varying H_2O_2 while maintaining constant the φ_{eff}, compression ratio and engine speed. These results are provided as a function of the compression ratio, for $\varphi_{eff} = 0.1$, 0.2, 0.3 and 0.4 and engine speeds of 1,000, 2000 and 3000 rpm. For all cases of engine speed a maximum quantity of 50% and 30% H_2O_2 was used at $\varphi = 0.1$ and 0.2, 0.3, 0.4, respectively. In certain cases, the required quantity of H_2O_2 to achieve the desired thermal efficiency exceeded the aforementioned H_2O_2 thresholds. Such cases, were at $\varphi_{eff} = 0.1$, compression ratio of 15 at 2000 rpm and compression ratio of 15 and 16 at 3000 rpm and at $\varphi_{eff} = 0.2$, compression ratio of 15 at 3000 rpm. At extremely lean conditions, i.e., $\varphi_{eff} = 0.1$, the use of H_2O_2 for ignition promotion purpose appears to be practical, i.e., ≤10% H_2O_2, at compression ratios of 17 or above, depending the engine speed (17 at 1000 rpm, 19 at 2000 rpm and 20 at 3000 rpm). At lower compression ratio values the required amount of H_2O_2 to achieve the desired thermal efficiency becomes significantly high. As the effective equivalence ratio increases to $\varphi_{eff} = 0.2$, the critical compression ratio decreases to 15 at 1000 rpm, 16.2 at 2000 rpm and 17 at 3000 rpm (i.e., above these values a 10% of H_2O_2 addition promotes sufficiently the system's ignition and results in the desired thermal efficiency). Increasing further the effective equivalence ratio to $\varphi_{eff} = 0.3$

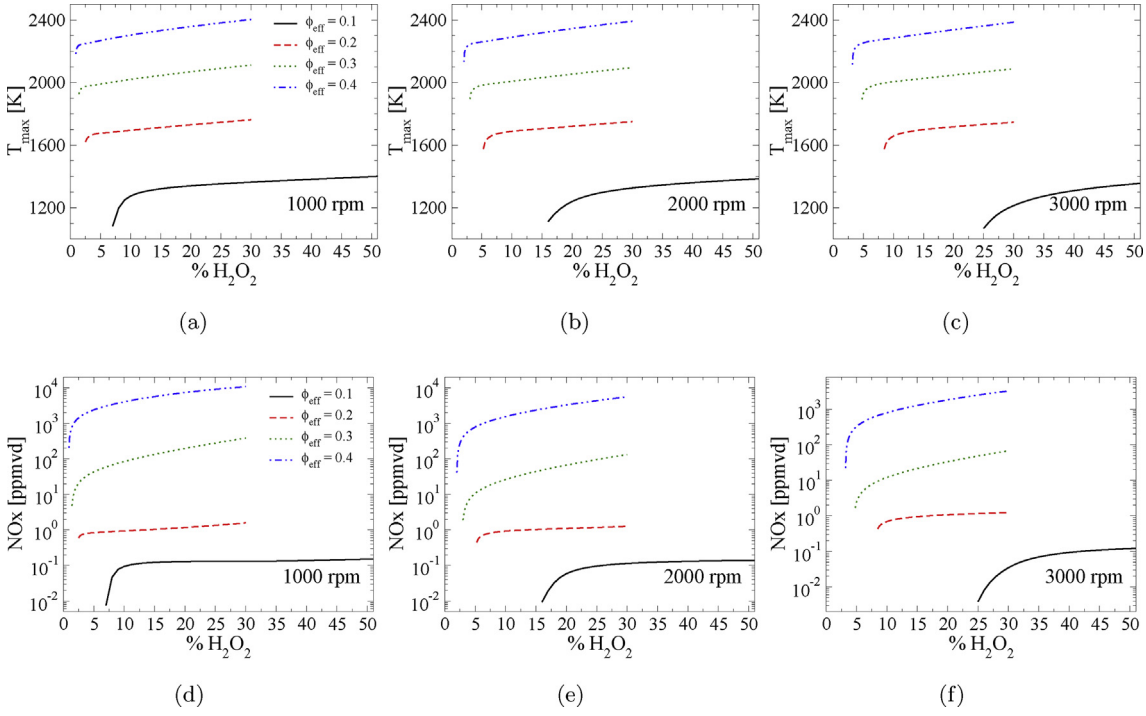

Fig. 7 – The variation of the maximum in-cylinder temperature (a–c) and NOx emissions (d–f) as a function of the H_2O_2 addition, for engine speed of (a, d) 1000, (b, e) 2000 and (c, f) 3000 rpm and equivalence ratios of $\varphi = 0.1$, 0.2, 0.3 and 0.4. The percentage of H_2O_2 addition refers to the H_2 mole fraction.

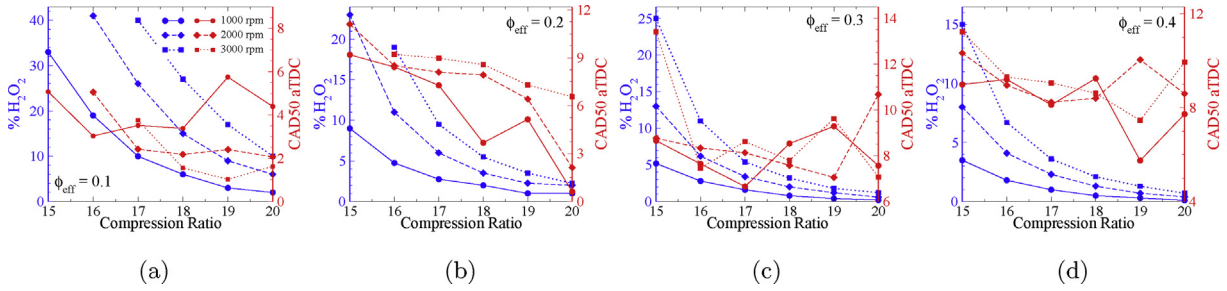

Fig. 8 – The variation of the percentage H_2O_2 addition required for thermal efficiency at the 98% of the maximum efficiency at constant φ_{eff}, engine speed and compression ratio. Also, the respective CAD for 50% of the heat release rate are displayed. The compression ratios vary between 15 and 20, the engine speeds are 1000, 2000 and 3000 rpm and the effective equivalence ratios are φ_{eff} = 0.1 (a), 0.2 (b), 0.3 (c) and 0.4 (d). The percentage of H_2O_2 addition refers to the H_2 mole fraction.

and 0.4, decreases further the critical compression ratio; at 1000 rpm the critical compression ratio value that requires 10% (or less) H_2O_2 addition to produce the desired thermal efficiency outcome is 15, at 2000 rpm that value becomes 16 and 15 for φ_{eff} = 0.3 and 0.4, respectively, and at 3000 rpm the critical compression ratio value is 16.5 (φ_{eff} = 0.3) and 15.5 (φ_{eff} = 0.4). All these results showcase the feasibility of the proposed use of H_2O_2 for ignition promotion purpose at extremely lean conditions (φ_{eff} = 0.1–0.2) and relatively high compression ratios, i.e., ≥17, since at lower compression ratios the required quantity of H_2O_2 to achieve ignition and high thermal efficiency increases greatly (> 10%). On the other hand, with richer mixtures (φ_{eff} = 0.3–0.4), the proposed technology produces high thermal efficiency outcomes with lower compression ratios (15.5–16.5) at all engine speeds. Unlike thermal efficiency, combustion phasing in view of CAD50 does not follow a monotonic trend with respect to the compression ratio change. Another striking difference compared to the thermal efficiency trend is that CAD50 generally varies little with the compression ratio, with potentially the only exception being the case of φ_{eff} = 0.2 at 1000 and 2000 rpm where there is a variation of roughly 9 CAD. Finally, it is worth noting that CAD50 in all cases vary between 0 and 14 CAD aTDC.

In the last part of the analysis, the effect of H_2O_2 addition on the engine performance, combustion phasing and NOx is explored, while maintaining constant the engine load. In particular, two scenarios are investigated: one representative of low load and a second one representing medium load. The torque at the low load conditions is maintained at 33.8 N•m while at medium load it is kept constant at 68.7 N•m. It is noted that the torque is maintained constant for all engine speeds. In order to meet the requirement for constant torque, two approaches are investigated and results are presented for both in Fig. 9 (low load) and 10 (medium load). In the first approach, while the initial H_2O_2 content in the H_2/air system is incrementally increased, the effective equivalence ratio is kept fixed (at 0.2 and 0.5 for low and medium loads, respectively) while the pressure intake is properly adjusted to maintain constant the torque. In the second approach, the pressure intake is kept fixed and the effective equivalence ratio is altered in order to conserve the torque constant. Of both approaches, the latter is easier to implement, although there is some room (yet limited) for implementation of the first one as well.

Fig. 9 showcases the strong effect of H_2O_2 addition, especially at 2000 and 3000 rpm. The change of the required intake pressure at 2000 rpm while decreasing the H_2O_2 addition from 10% to 8%–6% to 4%–2% is 1.3%, 2.2%, 47%, 235%, respectively while at 3000 rpm these changes become more pronounced: 5.8%, 58%, 110%, 169%, respectively. Notice the tremendous change in the intake pressure to maintain constant torque while decreasing the H_2O_2 percentage from 4% to 2%. The values of the required intake pressure at 2% H_2O_2 for both 2000 (5.5 bar) and 3000 (10.2 bar) are not shown in Fig. 9 because they have no practical value. The impact on the thermal efficiency is similarly strong. Decreasing the H_2O_2 addition from 10% to 8%–6% to 4%–2% at 2000 and 3000 rpm yields the following changes (decreases) in the thermal efficiencies: 0.3%, 1.1%, 31.2%, 69.8% and 4.5%, 36.1%, 51.8%, 62.5%. In essence, the H_2O_2 addition has a practical value for percentages equal or larger than 4% (P_{in} = 1.11 bar) at 1000 rpm, 6% (P_{in} = 1.12 bar) at 2000 rpm and 8% (P_{in} = 1.14 bar) at 3000 rpm, since below these values the thermal efficiency drops to very low figures.

On the other hand, in case of adjusting φ_{eff} instead of P_{in} to maintain constant torque while incrementally decreasing the initial percentage of H_2O_2 in the initial H_2/air mixture from 10% to 2% with a step of 2%, the required φ_{eff} increases 1.5%, 2.3%, 14.9%, 66.9% at 2000 rpm and 4.5%, 18.7%, 34.5%, 69.1% at 3000 rpm. These results indicate that φ_{eff} is more effective than the intake pressure in controlling torque, since the changes of φ_{eff} are smaller in magnitude. However, in view of the thermal efficiency although the induced changes are smaller in magnitude than the respective changes due to the adjustment of the intake pressure, the H_2O_2 addition has practical value for percentages equal or larger than 4% (φ_{eff} = 0.2068) at 1000 rpm, 6% (φ_{eff} = 0.2068) at 2000 rpm and 8% (φ_{eff} = 0.211) at 3000 rpm. This a conclusion that both approaches converge.

The great of impact of H_2O_2 addition is also manifested at the combustion phasing. At 1000 rpm increasing the H_2O_2 from 2% to 4% induces 23.9 CAD decrease of the CAD50, through the adjustment of the intake pressure. As the percentage of H_2O_2 increases a little further the CAD50 reaches values before the TDC. At 2000 rpm and for H_2O_2 content higher than 6% (the suitable quantity based on the thermal efficiency) CAD50 ranges between 1 and 8 CAD aTDC which are suitable for the HCCI engine operation. On the other hand,

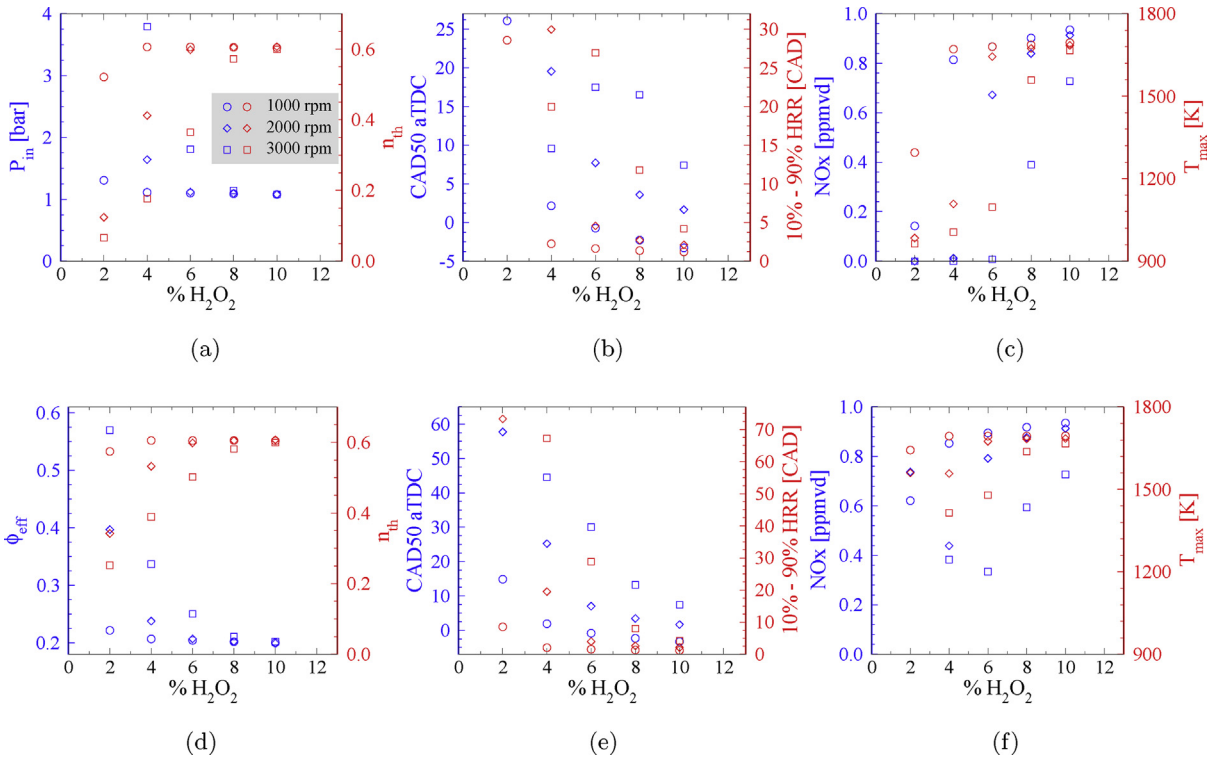

Fig. 9 – The effect of H_2O_2 addition on the thermal efficiency (a, d), the CAD for 50% of the heat release rate (b, e), the rapid burn angle, i.e., the CAD for 10%–90% heat release rate, (b, e), the NOx emissions (c, f) and the maximum temperature (c, f), at engine speeds of 1000, 2000 and 3000 rpm, while maintaining constant torque (33.8 N·m) through the adjustment of either the intake pressure (a–c) or the effective equivalence ratio (d–f). For the cases where torque is maintained constant through the adjustment of the intake pressure (a–c), the effective equivalence ratio is $\varphi_{eff} = 0.2$. The required intake pressure values as a function of the H_2O_2 addition are shown in (a). For the cases where torque is maintained constant through the adjustment of the effective equivalence ratio (d–f), the intake pressure is kept at 1 atm for all engine speeds. The required equivalence ratio values as a function of the H_2O_2 addition are shown in (d). The percentage of H_2O_2 addition refers to the H_2 mole fraction.

for H_2O_2 content higher than 8% (identified earlier as the minimum ideal quantity at 3000 rpm) CAD50 ranges between 7 (10% H_2O_2) and 17 (8% H_2O_2), the latter being considered unsuitable for HCCI engine operation. The rapid burn angle (RBA) results demonstrate that at 1000 rpm for H_2O_2 content higher than 2%, the RBA decreases to values in the order of 1–2 CAD. At 2000 rpm the RBA reaches values as low as 2 CAD for H_2O_2 content higher or equal to 8% while for H_2O_2 content lower or equal to 4% the RBA ranges between 18 and 30 CAD. Finally, at 3000 rpm the RBA is 4.2 and 11.8 CAD at 10% and 8% H_2O_2, which are both suitable for HCCI engine operation.

The variation of CAD50 with the adjustment of the effective equivalence ratio (Fig. 9e) is very similar to the approach of adjusting the intake pressure, previously described. In fact, the only striking differences are observed at very low H_2O_2 content (2%–4%) at all engine speeds. The same applies for the RBA, i.e., the results from the two approaches are very similar with the most pronounced differences being at low H_2O_2 content (2%–4%).

Both approaches also indicate that NOx emissions are extremely low (< 1 ppmvd) at all cases of H_2O_2 addition and engine speeds which is attributed to the generally low maximum temperatures (1500–1700 K) reached by the system in the engine cycle. These results highlight the potential of the proposed technology requiring no after-treatment for the NOx emissions at low loads.

At medium loads, the effect of H_2O_2 addition is less spectacular, which is due to the higher effective equivalence ratio that is used (0.5 compared to 0.2 at low loads). In fact, the variations between the minimum and maximum intake pressures (due to the different H_2O_2 contents) are 2.7%, 4.0% and 48% at 1,000, 2000 and 3000 rpm, respectively (comparatively, at low loads the respective values were 21%, 409% and 846%). The small variation of the intake pressures is reflected to the thermal efficiency which is consistently maintained at high values, between 54.1% and 56.4%, at all engine speeds. The only exception is at 3000 rpm and 2% H_2O_2, where thermal efficiency drops to 40%.

The respective results through the adjustment of the effective equivalence ratio while keeping the intake pressure fixed are very similar. The effective equivalence ratio exhibits 4.2%, 6.0% and 19.5% changes between their minimum and maximum values at the different engine speeds of 1,000, 2000 and 3000 rpm, respectively (comparatively, at low loads the respective values were 10.8%, 99.2% and 182%). In addition, the thermal efficiency is maintained at the same range of values (54% and 56%), with the only exception being the case of 3000 rpm and 2% H_2O_2 where thermal efficiency drops

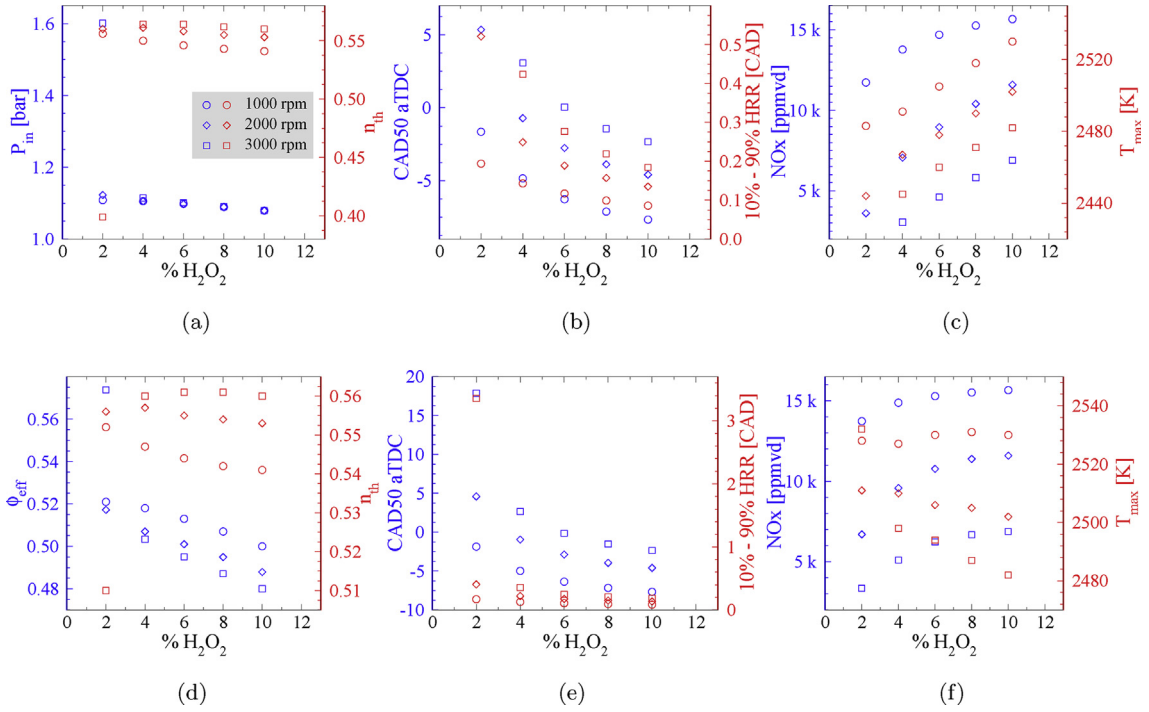

Fig. 10 – The effect of H_2O_2 addition on the thermal efficiency (a, d), the CAD for 50% of the heat release rate (b, e), the rapid burn angle, i.e., the CAD for 10%–90% heat release rate, (b, e), the NOx emissions (c, f) and the maximum temperature (c, f), at engine speeds of 1000, 2000 and 3000 rpm, while maintaining constant torque (68.7 N·m) through the adjustment of either the intake pressure (a–c) or the effective equivalence ratio (d–f). For the cases where torque is maintained constant through the adjustment of the intake pressure (a–c), the effective equivalence ratio is $\varphi_{eff} = 0.5$. The required intake pressure values as a function of the H_2O_2 addition are shown in (a). For the cases where torque is maintained constant through the adjustment of the effective equivalence ratio (d–f), the intake pressure is kept at 1 atm for all engine speeds. The required equivalence ratio values as a function of the H_2O_2 addition are shown in (d). The percentage of H_2O_2 addition refers to the H_2 mole fraction.

significantly (51%) as it was described earlier with the adjustment of the intake pressure.

The results on high load conditions so far indicate that a mere 2%–4% H_2O_2 addition would be sufficient to maintain constant load at all investigated engine speeds. However, the examination of CAD50 in Fig. 10b and e illustrates the substantial ignition advancement achieved by the addition of H_2O_2 leading it rapidly to values relevant to bTDC. Also, both approaches (adjusting P_{in} or φ_{eff}) exhibit extremely fast rapid burn angles (<1 CAD) at all engine speeds, with the only exception that of 3000 rpm and 2% H_2O_2 addition in the case of adjusting φ_{eff} (Fig. 10e). Based on these results, it can be concluded that the ideal quantities of H_2O_2 to maintain constant medium load are 2%, 4% and 6% at engine speeds of 1,000, 2000 and 3000 rpm, respectively.

The same consistency of the results between the two approaches (adjusting P_{in} or φ_{eff}) is roughly maintained for the NOx emissions as well as the maximum temperatures. However, different to the low load case where it was showcased the negligible NOx emissions production, at medium load conditions NOx emissions reach extremely high values, ranging between 11,000–16,000, 3,500k-12,000 and 3000–7000 for engine speeds of 1,000, 2000 and 3000 rpm, respectively. These high NOx emission values are inherently due to the high temperature values reached by the system due to the significantly more fuel rich conditions compared to the low load cases. Indicatively, the maximum temperatures reached at the high load conditions are 2,483K-2,531 K, 2444–2,502 K, 2,021K-2,532 K, for engine speeds of 1,000, 2000 and 3000 rpm, respectively (comparatively, at low loads the average maximum temperature considering all engine speeds was 1,537 K). These results indicate that the use of H_2O_2 for ignition promotion purposes while at low load conditions leads to extremely low NOx emissions, at medium loads some after treatment or low combustion strategy (e.g., steam addition) would be required to tackle with the high NOx emissions.

Conclusions

In this work, the addition of H_2O_2 in hydrogen fueled HCCI was showcased numerically, using a simplified commercial model (Chemkin-Pro). The proposed technology aims to enable the use of hydrogen in CI-type engines with direct application on heavy duty vehicles and ships, which are currently difficult to decarbonise. With the understanding that the employed simplified engine model has inherent limitations, the objective of the current work was to examine its feasibility in view of engine performance characteristics, combustion phasing and NOx emissions and to identify trends and qualitative

features of the H_2O_2 addition. The results described herein are promising and numerical evidence of the benefits of the proposed technology are provided.

In particular:

- the comparison of the proposed use of hydrogen/hydrogen peroxide blends against the sufficient preheating of hydrogen/air blends at extremely lean conditions indicated that the first can lead to significant increase of the IMEP, the indicated power and torque, small increase of the thermal efficiency, notable decrease of the maximum temperature and tremendous decrease of NOx emissions. The only caveat was some small increase of the maximum pressure. As the mixture becomes richer, the increase on the engine performance characteristics becomes less pronounced while the decrease of NOx emissions is maintained high.
- the addition of H_2O_2 indicated a strong ignition advancement at all conditions. 10% H_2O_2 addition (with $\varphi_{eff} = 0.1–0.4$, depending the engine speed) was sufficient to advance the ignition CAD to values close to zero aTDC and lead to RBA values less than 4 CAD, at all engine speeds.
- the effect of H_2O_2 addition on the combustion phasing becomes significantly less pronounced as the system becomes leaner.
- the addition of H_2O_2 increases the IMEP, power, torque for all engine speeds and extremely lean effective equivalence ratios. As the mixture becomes richer the effect of H_2O_2 addition on IMEP, power and torque becomes stronger at a gradually smaller rate.
- the addition of H_2O_2 highlighted the system's tendency to increase the thermal efficiency, regardless the engine speed and the effective equivalence ratio. Also, the thermal efficiency can exceed values of 60% at sufficiently lean conditions through some small ($\leq$10%) addition of H_2O_2.
- at sufficiently low effective equivalence ratios, e.g., $\varphi_{eff} = 0.1$ or 0.2, H_2O_2 addition leads to extremely low NOx emissions ($\leq$1.5 ppmvd), so low that would not require any after-treatment. However, for $\varphi_{eff} > 0.2$ NOx emissions increase rapidly and reach values which may necessitate after-treatment or the use of additional strategies to combat the increased emissions, such as the use water/steam.
- the use of H_2O_2 for ignition promotion purpose at extremely lean conditions ($\varphi_{eff} = 0.1–0.2$) is favored at relatively high compression ratios, i.e., $\geq$17, since at lower compression ratios the required quantity of H_2O_2 to achieve ignition and high thermal efficiency increases greatly (>10%). On the other hand, with richer mixtures ($\varphi_{eff} = 0.3–0.4$), the proposed technology produces high thermal efficiency outcomes with lower compression ratios (15.5–16.5) at all engine speeds.

The above results are promising but further numerical and experimental research is required to actively further demonstrate the feasibility of the proposed technology.

Declaration of competing interest

The authors declare that they have no known competing financial interests or personal relationships that could have appeared to influence the work reported in this paper.

vAcknowledgments

The work of EAT was supported by the EPSRC Network-H_2 through Flexible Fund grant scheme with Grant No. RF080413 (NH2-006).

REFERENCES

[1] Fayaz H, Saidur R, Razali N, Anuar F, Saleman A, Islam M. An overview of hydrogen as a vehicle fuel. Renew Sustain Energy Rev 2012;16(8):5511–28.
[2] Oliveira AM, Beswick RR, Yan Y. A green hydrogen economy for a renewable energy society. Curr Opin Chem Eng. 2021;33:100701.
[3] Sharma S, Ghoshal SK. Hydrogen the future transportation fuel: from production to applications. Renew Sustain Energy Rev 2015;43:1151–8.
[4] Megía PJ, Vizcaíno AJ, Calles JA, Carrero A. Hydrogen production technologies: from fossil fuels toward renewable sources. a mini review. Energy Fuels 2021;35(20):16403–15.
[5] Hydrogen and Fuel Cell Strategy Council, The strategic roadmap for hydrogen and fuel cells.
[6] UK Government BEIS. The energy white paper, powering our net zero future. 2020CP337.
[7] Das L. Hydrogen engines: a view of the past and a look into the future. Int J Hydrogen Energy 1990;15(6):425–43.
[8] Karim GA. Hydrogen as a spark ignition engine fuel. Int J Hydrogen Energy 2003;28(5):569–77.
[9] Verhelst S, Sierens R, Verstraeten S. A critical review of experimental research on hydrogen fueled SI engines. SAE Trans 2006:264–74.
[10] Verhelst S. Recent progress in the use of hydrogen as a fuel for internal combustion engines. Int J Hydrogen Energy 2014;39(2):1071–85.
[11] Stepien Z. A comprehensive overview of hydrogen-fueled internal combustion engines: achievements and future challenges. Energies 2021;14(20):6504.
[12] Shadidi B, Najafi G, Yusaf T. A review of hydrogen as a fuel in internal combustion engines. Energies 2021;14(19):6209.
[13] Stockhausen WF, Natkin RJ, Kabat DM, Reams L, Tang X, Hashemi S, Szwabowski SJ, Zanardelli VP. Ford P2000 Hydrogen engine design and vehicle development program. SAE Tech Pap 2002. https://doi.org/10.4271/2002-01-0240.
[14] Taxon MN, Brueckner SR, Bohac SV. Effect of fuel humidity on the performance of a single-cylinder research engine operating on hydrogen. SAE Trans 2002:1194–213.
[15] Rottengruber H, Berckmüller M, Elsässer G, Brehm N, Schwarz C. Direct-injection hydrogen SI-engine-operation strategy and power density potentials. SAE Trans 2004:1749–61.
[16] Homan H, Reynolds R, De Boer P, McLean W. Hydrogen-fueled diesel engine without timed ignition. Int J Hydrogen Energy 1979;4(4):315–25.
[17] Aleiferis PG, Rosati MF. Controlled autoignition of hydrogen in a direct-injection optical engine. Combust Flame 2012;159(7):2500–15.

[18] Welch A, Wallace J. Performance characteristics of a hydrogen-fueled diesel engine with ignition assist. SAE Tech Pap 1990. https://doi.org/10.4271/902070.
[19] Stenlåås O, Christensen M, Egnell R, Johansson B, Mauss F. Hydrogen as homogeneous charge compression ignition engine fuel. SAE Trans 2004:1317–26.
[20] Antunes JG, Mikalsen R, Roskilly A. An investigation of hydrogen-fuelled HCCI engine performance and operation. Int J Hydrogen Energy 2008;33(20):5823–8.
[21] Antunes JG, Mikalsen R, Roskilly A. An experimental study of a direct injection compression ignition hydrogen engine. Int J Hydrogen Energy 2009;34(15):6516–22.
[22] Caton P, Pruitt J. Homogeneous charge compression ignition of hydrogen in a single-cylinder diesel engine. Int J Engine Res 2009;10(1):45–63.
[23] Ibrahim MM, Ramesh A. Experimental analysis of hydrogen-fueled homogeneous charge compression ignition (HCCI) engine. In: Exergy for A Better environment and improved sustainability 2. Springer; 2018. p. 471–87.
[24] Bika AS, Franklin L, Acevedo H, Kittelson D. Hydrogen fueled homogeneous charge compression ignition engine. SAE Techn. Pap; 2011.
[25] Dimitriou P, Tsujimura T. A review of hydrogen as a compression ignition engine fuel. Int J Hydrogen Energy 2017;42(38):24470–86.
[26] Tsujimura T, Suzuki Y. The utilization of hydrogen in hydrogen/diesel dual fuel engine. Int J Hydrogen Energy 2017;42(19):14019–29.
[27] Dimitriou P, Tsujimura T, Suzuki Y. Adopting biodiesel as an indirect way to reduce the nox emission of a hydrogen fumigated dual-fuel engine. Fuel 2019;244:324–34.
[28] Li L, Yu Y, Lin W. Numerical investigation on the effects of load conditions and hydrogen-air ratio on the combustion processes of a hsdi engine. Int J Hydrogen Energy 2020;45(17):10602–12.
[29] Rakopoulos C, Scott M, Kyritsis D, Giakoumis E. Availability analysis of hydrogen/natural gas blends combustion in internal combustion engines. Energy 2008;33(2):248–55.
[30] Tarabet L, Lounici M, Loubar K, Khiari K, Bouguessa R, Tazerout M. Hydrogen supplemented natural gas effect on a di diesel engine operating under dual fuel mode with a biodiesel pilot fuel. Int J Hydrogen Energy 2018;43(11):5961–71.
[31] Boretti AA. Novel heavy duty engine concept for operation dual fuel H2–NH3. Int J Hydrogen Energy 2012;37(9):7869–76.
[32] Seignour N, Masurier J, Johansson B, Dayma G, Dagaut P, Foucher F. Ozone-assisted combustion of hydrogen: a comparison with isooctane. Int J Hydrogen Energy 2019;44(26):13953–63.
[33] Tingas E-A. The chemical dynamics of hydrogen/hydrogen peroxide blends diluted with steam at compression ignition relevant conditions. Fuel 2021;296:120594.
[34] Tingas E-A. Computational analysis of the effect of hydrogen peroxide addition on premixed laminar hydrogen/air flames. Fuel 2021;302:121081.
[35] Amri R, Rezoug T. Numerical study of liquid propellants combustion for space applications. Acta Astronaut 2011;69(7–8):485–98.
[36] Lestrade J-Y, Anthoine J, Musker AJ, Lecossais A. Experimental demonstration of an end-burning swirling flow hybrid rocket engine. Aero Sci Technol 2019;92:1–8.
[37] Ashok M, Saravanan C. Role of hydrogen peroxide in a selected emulsified fuel ratio and comparing it to diesel fuel. Energy Fuels 2008;22(3):2099–103.
[38] Gribi B, Lin Y, Hui X, Zhang C, Sung C-J. Effects of hydrogen peroxide addition on combustion characteristics of n-decane/air mixtures. Fuel 2018;223:324–33.
[39] Anufriev I. Review of water/steam addition in liquid-fuel combustion systems for nox reduction: waste-to-energy trends. Renew Sustain Energy Rev 2021;138:110665.
[40] Zhang C, Wu H. The simulation based on chemkin for homogeneous charge compression ignition combustion with on-board fuel reformation in the chamber. Int J Hydrogen Energy 2012;37(5):4467–75.
[41] Zhang Z, Xie Q, Liang J, Li G. Numerical study of combustion characteristics of a natural gas hcci engine with closed loop exhaust-gas fuel reforming. Appl Therm Eng 2017;119:430–7.
[42] Wang Y, Zhou X, Liu L. Theoretical investigation of the combustion performance of ammonia/hydrogen mixtures on a marine diesel engine. Int J Hydrogen Energy 2021;46(27):14805–12.
[43] Heywood JB. Internal combustion engine fundamentals. McGraw-Hill Education; 2018.
[44] Design R. ANSYS Chemkin theory manual 21.0. 2021.
[45] Zhou C-W, Li Y, Burke U, Banyon C, Somers KP, Ding S, Khan S, Hargis JW, Sikes T, Mathieu O, et al. An experimental and chemical kinetic modeling study of 1, 3-butadiene combustion: ignition delay time and laminar flame speed measurements. Combust Flame 2018;197:423–38.
[46] Glarborg P, Miller JA, Ruscic B, Klippenstein SJ. Modeling nitrogen chemistry in combustion. Prog Energy Combust Sci 2018;67:31–68.
[47] Hui X, Zheng D, Zhang C, Xue X, Sung C-J. Effects of hydrogen peroxide addition on two-stage ignition characteristics of n-heptane/air mixtures. Int J Hydrogen Energy 2019;44(44):24312–20.
[48] Maurya RK, Saxena MR. Characterization of ringing intensity in a hydrogen-fueled HCCI engine. Int J Hydrogen Energy 2018;43(19):9423–37.
[49] Ibrahim MM, Ramesh A. Investigations on the effects of intake temperature and charge dilution in a hydrogen fueled hcci engine. Int J Hydrogen Energy 2014;39(26):14097–108.